Original Article

Whole-Genome and Transcriptome Sequencing Identified *NOTCH2* and *HES1* as Potential Markers of Response to Imatinib in Desmoid Tumor (Aggressive Fibromatosis): A Phase II Trial Study

Joonha Kwon [1], Jun Hyeong Lee [1], Young Han Lee[2], Jeeyun Lee[3], Jin-Hee Ahn[4], Se Hyun Kim[5], Seung Hyun Kim[6], Tae Il Kim[7], Kum-Hee Yun[8], Young Suk Park[3], Jeong Eun Kim[4], Kyu Sang Lee[9], Jung Kyoon Choi [1], Hyo Song Kim [8,10]

[1]Department of Bio and Brain Engineering, Korea Advanced Institute of Science and Technology (KAIST), Daejeon, [2]Department of Radiology, Yonsei University College of Medicine, Seoul, [3]Division of Hematology-Oncology, Department of Medicine, Samsung Medical Center, Sungkyunkwan University School of Medicine, Seoul, [4]Department of Oncology, Asan Medical Center, University of Ulsan College of Medicine, Seoul, [5]Division of Hematology and Medical Oncology, Department of Internal Medicine, Seoul National University Bundang Hospital, Seongnam, [6]Department of Orthopedic Surgery, Yonsei University College of Medicine, Seoul, [7]Division of Gastroenterology, Department of Internal Medicine, Yonsei University College of Medicine, Seoul, [8]Brain Korea 21 PLUS Project for Medical Science, Yonsei University College of Medicine, Seoul, [9]Department of Pathology, Seoul National University Bundang Hospital, Seongnam, [10]Division of Medical Oncology, Department of Internal Medicine, Yonsei University College of Medicine, Seoul, Korea

Purpose Desmoid tumor, also known as aggressive fibromatosis, is well-characterized by abnormal Wnt/β-catenin signaling. Various therapeutic options, including imatinib, are available to treat desmoid tumor. However, the molecular mechanism of why imatinib works remains unclear. Here, we describe potential roles of *NOTCH2* and *HES1* in clinical response to imatinib at genome and transcriptome levels.

Materials and Methods We identified somatic mutations in coding and noncoding regions via whole-genome sequencing. To validate the genetic interaction with expression level in desmoid-tumor condition, we utilized large-scale whole-genome sequencing and transcriptome datasets from the Pan-Cancer Analysis of Whole Genomes project. RNA-sequencing was performed using prospective and retrospective cohort samples to evaluate the expressional relevance with clinical response.

Results Among 20 patients, four (20%) had a partial response and 14 (66.7%) had stable disease, 11 of which continued for ≥ 1 year. With gene-wise functional analyses, we detected a significant correlation between recurrent *NOTCH2* noncoding mutations and clinical response to imatinib. Based on Pan-Cancer Analysis of Whole Genomes data analyses, *NOTCH2* mutations affect expression levels particularly in the presence of *CTNNB1* missense mutations. By analyzing RNA-sequencing with additional desmoid tumor samples, we found that *NOTCH2* expression was significantly correlated with *HES1* expression. Interestingly, *NOTCH2* had no statistical power to discriminate between responders and non-responders. Instead, *HES1* was differentially expressed with statistical significance between responders and non-responders.

Conclusion Imatinib was effective and well tolerated for advanced desmoid tumor treatment. Our results show that *HES1*, regulated by *NOTCH2*, as an indicator of sensitivity to imatinib, and an important therapeutic consideration for desmoid tumor.

Key words Fibromatosis aggressive, Imatinib mesylate, Clinical trial phase II, Computational biology, Whole-genome sequencing, Transcriptome

Introduction

A desmoid tumor (aggressive fibromatosis) is a fibroproliferative neoplasm arising from deep connective tissues. A stepwise approach including active surveillance is established as no metastatic potential and spontaneous tumor regression are observed [1]. Excision is the mainstay of treatment, but the postsurgical recurrence rate is high [2,3]. For unresectable or recurrent desmoid tumors, a variety of systemic therapeutic options are available, including tamoxifen, nonsteroidal anti-inflammatory drugs (NSAIDs), interferons, and chemotherapy [4-8]. Recently, sorafenib induced durable response and led to its approval for the disease treatment [9]. Imatinib is a new treatment option in unresectable, progressive, or recurrent desmoid tumors [10-12]. In addition to its promising efficacy (6%-15% response rate), the favorable tox-

icity profiles support its long-term use for salvage treatment. In imatinib-responsive diseases, such as gastrointestinal stromal tumors or chronic myeloid leukemia, specific mutations or chromosomal translocations have been reported [13-15]. However, in desmoid tumors, no molecular abnormalities in imatinib-sensitive kinases have been observed [10,11]. Therefore, molecular mechanisms by which this rare tumor responds to imatinib are poorly understood.

In this study, we conducted a multicenter phase II trial to evaluate the efficacy of imatinib in patients with relapsing or progressive desmoid tumors (ClinicalTrials.gov, NCT02495519, registered July 13, 2015 retrospectively registered). To understand the molecular basis of the clinical responses to imatinib, we performed whole-genome sequencing to identify potential markers. Owing to limited insights gained from protein-coding mutations, we extended our analyses to noncoding regulatory regions. Our gene-wise recurrence model using 1,009 pan-cancer whole-genome data indicated that *NOTCH2* regulatory mutations are associated with the response of desmoid tumors to imatinib. We further evaluated the significance of *NOTCH2* in transcriptome analysis using RNA-sequencing data. We discovered that *HES1*, a well-known downstream target of Notch signaling pathway, is directly associated with imatinib sensitivity.

Materials and Methods

1. Patients and treatment

Patients with advanced desmoid tumors, defined as patients with radiographic progression after previous treatment, were eligible for prospective phase II study. Key inclusion criteria were as follows: age ≥ 10 years, Eastern Cooperative Oncology Group performance status of 0 to 2, and adequate hematologic and renal function. Patients were treated with 400 mg of imatinib mesylate (Glima, Boryung Pharmaceutical Co., Ltd., Seoul, Korea) daily until progression or unacceptable toxicity. Toxic effects were graded according to the National Cancer Institute—Common Toxicity Criteria v. 4.03. Disease was assessed every 8 weeks for the initial 32 weeks and then every 16 weeks according to RECIST (Response Evaluation Criteria in Solid Tumors) v1.1 [16]. Briefly, patients who experienced grade 3/4 toxicity or intolerable grade 2 toxicity stopped treatment and then restarted at a reduced dose (300 mg/day or 200 mg/day). Surgically resected formalin-fixed paraffin-embedded (FFPE) tissue samples obtained prior to radiotherapy or chemotherapy were subjected to transcriptome sequencing (Fig. 1). Of those, four cases were treated with imatinib and the remaining 20 were treatment naïve.

2. DNA extraction and quality assessment

Whole genome sequencing was performed using pretreatment tumor excision samples as well as matched blood samples. Briefly, 4-mm-thick sections with a tumor content of ≥ 80% were obtained, and ≥ 2 µg of DNA was extracted using the Maxwell 16 FFPE Plus LEV DNA Purification Kit (Promega, Madison, WI). For peripheral blood mononuclear cells (PBMCs), genomic DNA was extracted using the QIAamp DNA Mini Kit (Qiagen, Hilden, Germany) as per the manufacturer's instructions.

3. DNA library construction and whole-genome sequencing

Library preparation was performed using the TruSeq Nano DNA Library Preparation Kit (Illumina, San Diego, CA) following the manufacturer's instructions. Illumina utilizes a unique "bridged" amplification reaction on the surface of the flow cell. A flow cell containing libraries was prepared using the cBot Fluidics Station and was then loaded into the HiSeq X-10 sequencer (Illumina) for automated cycles of extension and imaging. Sequencing-by-Synthesis cycles were repeated to achieve a paired-end read length of 2×150 bp.

4. RNA library construction and whole transcriptome sequencing

Total RNAs were extracted and purified from frozen tumor samples with ReliaPrep FFPE Total RNA Miniprep System (Promega) according to the manufacturer's procedures. Amount of RNA and its quality were checked on an Agilent RNA 6000 Nano Kit (Agilent Technologies, Santa Clara, CA). For analysis of RNA-sequencing data, we prepared mRNA sequencing libraries as paired-end reads with a length of 100 bases using the SMARTer Stranded Total RNA-seq kit v2-Pico Input Mammalian according to the manufacturers' protocols. Briefly, mRNA molecules were purified and fragmented from 2 µg of total RNA. The libraries were sequenced as paired-end reads (2×150 bp) using the NovaSeq 6000 (Illumina).

5. Whole genome data processing

To process whole-genome sequencing data of desmoid tumors, we adopted the Genome Analysis Tool Kit (GATK) v3.7 best practice provided by the Broad Institute [17]. Briefly, we mapped qualified paired-end reads to the human reference genome (hg19) with Burrows-Wheeler Aligner 0.7.15 [18]. Subsequently, we filtered polymerase chain reaction duplicates using Picard tools 2.8.2 to remove potential bias that occurred during sequencing processes. Then, we performed recommended procedures, such as local realignment and base quality recalibration to extract analysis-ready reads.
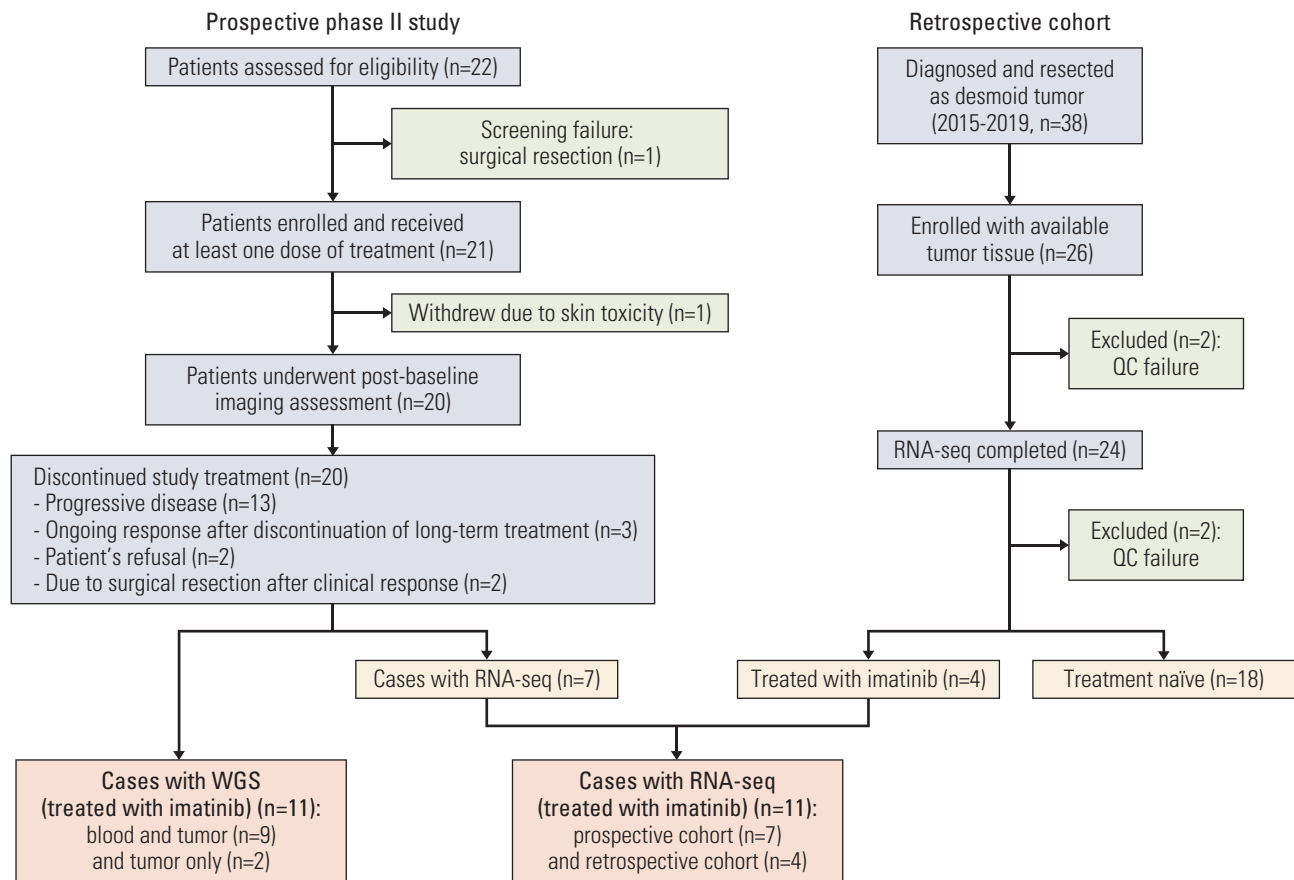
Fig. 1. Consort diagram of desmoid tumor patients included in this study. Prospective phase II study with treatment of imatinib included 20 patients after excluding two patients with clinical concerns. Tumor samples from 11 patients, which passed stringent quality check, were whole-genome-sequenced. RNA-sequencing (RNA-seq) was performed for 29 cases, including seven in phase II study and 22 in retrospective cohort, of which 11 cases were treated with imatinib. QC, quality control; WGS, whole-genome sequencing.

6. Somatic variant detection

MuTect2 [19] of the GATK pipeline with default parameters was used to identify somatic single nucleotide variants (SNVs) and small insertions/deletions (indels). The processed whole-genome-sequencing data for tumor and matched normal samples (PBMCs) were used in BAM format as inputs for Mutect2 [19]. Somatic variants were annotated using ANNOVAR [20]. Some candidate variants were manually inspected using Integrative Genomics Viewer [21]. Population-level allele frequencies of candidates were obtained using Genome Aggregation Database (gnomAD) [22]. For two samples with tumor data only, normal sample data for one of the nine other patients was used as matched normal control for variant calling. A sample that was sequenced in the same batch with a read depth of greater than 30 was used. The variants were further filtered using gnomAD to obtain putative somatic mutations in the tumor-only samples.

7. Scoring gene-wise recurrence of functional variants

Our previously developed gene-wise recurrence model was used [23]. Conventionally, mutations are considered recurrent if and only if they occur at the same genomic location across multiple samples. Mutations are considered oncogenic when their recurrence exceeds a certain threshold [24]. However, this definition of recurrence is inappropriate for analyses of noncoding regions owing to their vast size. Thus, we consider mutations recurrent if they occur in functional regions of the same gene, even if they are not recurrent in a site-specific manner. In particular, we focused on mutational events in cis-regulatory regions of a mammalian gene dispersed across a long range in the genome [25]. Genes were defined based on the GENCODE v.19 gene set mapped to GRCh37 [26].

To identify coding and noncoding mutations with significant functional consequences, deleterious effects of each SNV were predicted using two algorithms, Combined

Annotation-Dependent Depletion (CADD) [27] and Deleterious Annotation of genetic variants using Neural Networks (DANN) [28]. Both models were trained to distinguish benign variants from deleterious variants [27,28]. For multiple mutations in the same gene, the one with the highest score for deleteriousness was selected to represent the functional consequence.

8. Reference whole-genome and transcriptome datasets

To characterize the functional effects of *NOTCH2* noncoding mutations, a large-scale pan-cancer dataset consisting of somatic variants from whole-genome sequencing data and transcriptome data for tumor and matched normal samples were used. VCF files for somatic variant calling and gene expression matrices containing FPKM (fragments per kilobase of transcript per million mapped reads)-upper quantile values were obtained from the Pan-Cancer Analysis of Whole Genomes (PCAWG) Project [29].

9. RNA-sequencing data processing and quality control

We generated RNA-sequencing data of 31 desmoid tumor patients. We removed adapter sequences using Cutadpt [30], and aligned the trimmed reads using STAR [31] with hg19. Gene expression was quantified using RSEM [32]. Quality control check at pre-alignment step was conducted using FASTQC and at post-alignment step using RSeQC [33]. Quality control (QC) results were visualized with MultiQC [34]. At post-alignment step, we noticed two patients with potential problems in read distribution, and infer experiment criteria. Thus, we excluded those samples from future analysis.

10. Bioinformatics and statistical analyses

The chi-square test was used to assess correlations between marker status and clinical significance. All correlation analysis was conducted using spearman correlation. To assess statistical significance between responders and non-responders of imatinib, we calculated Mann-Whitney U test. All tests were two-sided and $p < 0.05$ is considered significant. Cleveland, scatter and box plots were generated by using ggplot2 R package and matplotlib python package.

To conduct enrichment analysis, we adopted two approaches. First of all, we identified genes that are significantly correlated with imatinib sensitivity and used those genes as input for EnrichR [35]. As an alternative step, we conducted Gene Set Enrichment Analysis (GSEA) between responders and non-responders using C2, C5, C6, and Hallmark MSigDB gene sets [36]. C5 Notch category was defined as Notch-related terms present in C5 category.

Progression-free survival was calculated from start date of imatinib to date of progression or death and progression-free rate at 16 weeks (PFR 16) was defined as proportions of patients without progression at 16 weeks, analyzed using the Kaplan-Meier method (SPSS ver. 18.0, SPSS Inc., Chicago, IL).

Results

1. Sample set, patient outcomes, and toxicity

Total of 21 patients was enrolled between April 2014 and October 2015. One patient withdrew, leaving 20 patients (Fig. 1, S1 Table). Three patients (7, 8, and 13) had a known diagnosis of familial adenomatous polyposis (FAP). Fifteen patients (75%) underwent one previous surgery. Most of the patients had been treated with non-surgical procedures, including radiotherapy (n=6, 30.0%) and/or chemotherapy (n=12, 60.0%).

Of the 20 evaluable patients, four (20%) had partial responses (PR) to treatment with durations of 6.7, 26.8 (Fig. 2A), 30.3, and 35.1 (Fig. 2B) months. One PR case had FAP. The PR duration was longer than 1 year for three patients. Fig. 2C provides a waterfall plot of the best response; 14 patients (66.7%) had stable disease (SD), and the clinical benefit rate was 90.0%. The median time to progression was 21.4 months (range, 2.8 to 40.7 months) and PFR 16 was 85% (Fig. 2D).

In terms of toxicity, 400 mg of imatinib was well tolerated with expected grade 3/4 toxicities: neutropenia (n=1), anorexia (n=1), vomiting (n=1), and fatigue (n=1) (S2 Table). Three patients had a one dose level reduction (300 mg/day), and one patient had a reduction of two levels (200 mg/day) owing to toxicity.

2. Results of whole-genome sequencing

After confirming adequate DNA quantities, whole genome sequencing was performed for 11 samples. Two samples (patients 11 and 13) without matched control data were excluded from the primary analysis and used for extensional validation only (Fig. 1). The average read depth was greater than 21.46 (range, 21.46 to 54.05) (S3 Table). By implementing the GATK pipeline from the Broad Institute, we identified 832-4,110 SNVs and indels per sample and used ANNOVAR for annotation (S4 Table).

Next, we examined mutational signatures from annotated variants to identify types of mutational processes [37]. Signature 1A was dominant, accounting for around 88% of signatures (S5 Table), indicating that desmoid tumor variants primarily arise due to errors in replicative polymerases in the DNA repair pathway [37]. The majority of mutations were in intronic regions. Mutations in coding regions were primarily missense and synonymous variants (S6 Fig.).

We also investigated alterations of cancer driver genes registered in the COSMIC database [38] and detected *CTNNB1*
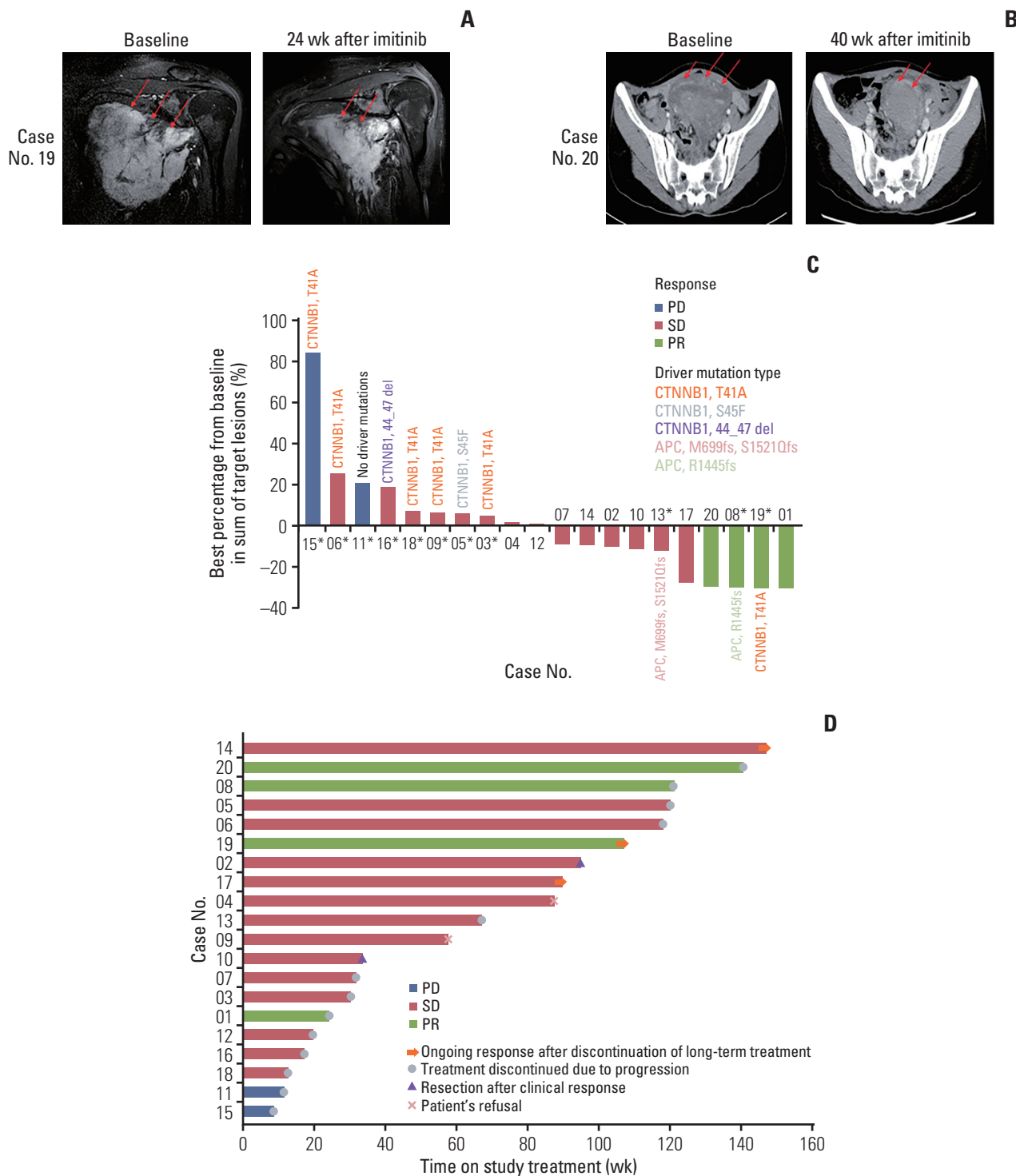
Fig. 2. Representative pre- and post-treatment imaging scans to show antitumor activity of imatinib in desmoid tumors. Soft tissue lesion in the shoulder of patient 19 (A) and pelvis of patient 20 (B) exhibited a significant size reduction after 24 and 40 weeks of imatinib treatment (red arrow). (C) Relative change in tumor volume of patients (n=20) over time. Asterisk indicates a sample with whole-genome sequencing data. The label at the end of the bar shows mutational information in known driver genes, *CTNNB1* and *APC*, for desmoid tumor. (D) Swimmer plot. Each lane represents a single patient's data. X-axis represents the duration of treatment for each patient. PD, progressive disease; PR, partial response; SD, stable disease.
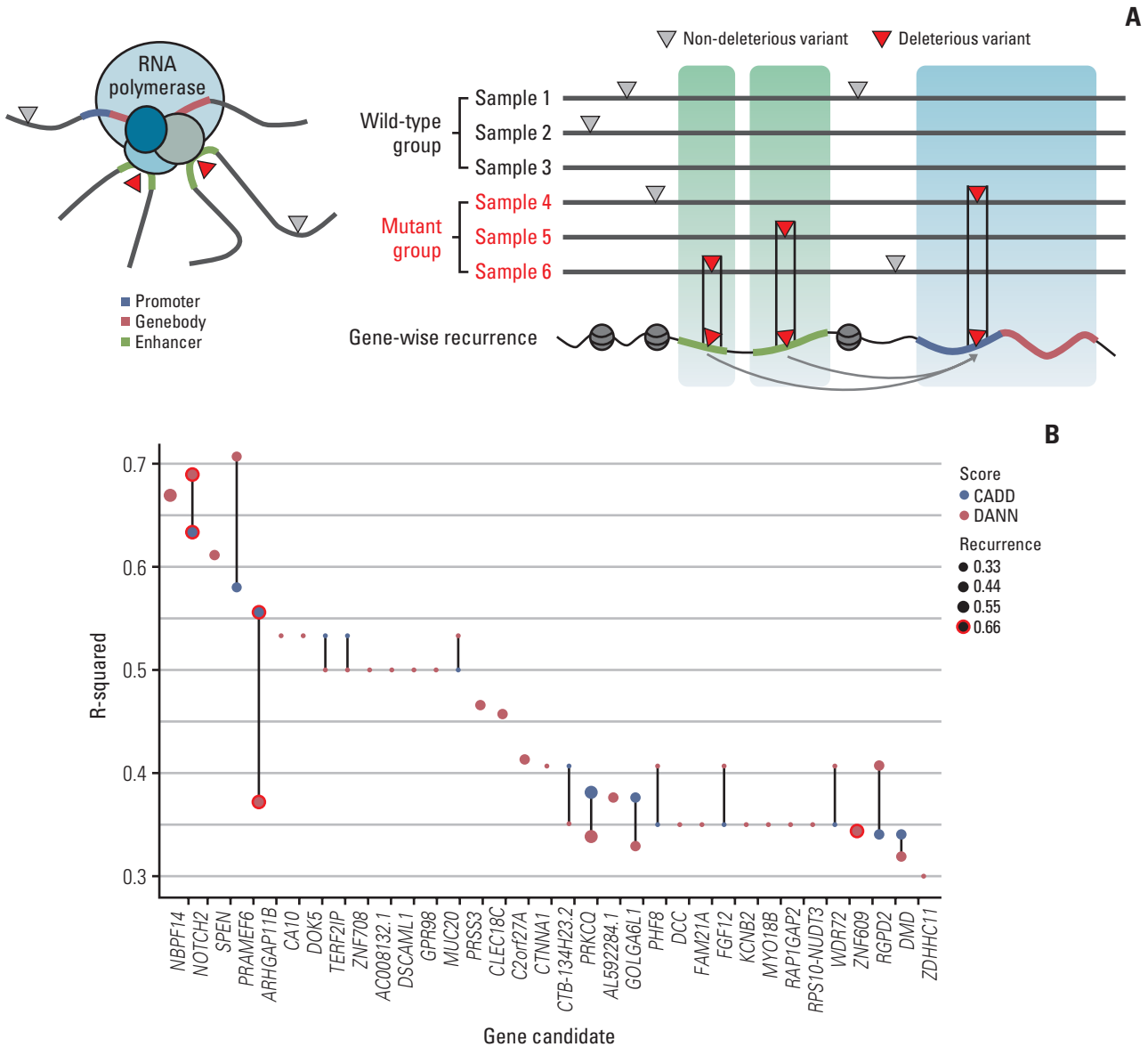
Fig. 3. Gene-wise recurrence of noncoding mutations. (A) Definition of functional noncoding mutations and schematic overview of the gene-wise recurrence model. Functional noncoding mutations in regulatory regions, such as enhancers, affect the expression level of the target gene. Mutations outside of functional regions were excluded from our analysis. Functional mutations were identified as recurrent if they occur in regulatory regions converging of the same gene via enhancer-promoter chromatin interactions across multiple patients. Deleteriousness of functional mutations in mutant groups was quantified using Combined Annotation-Dependent Depletion (CADD) and Deleterious Annotation of genetic variants using Neural Networks (DANN). (B) Cleveland plot shows correlation coefficients (R^2) for the relationship between tumor volume change and deleteriousness score, and recurrence for each gene in desmoid tumor patients (n=9). Genes are ordered by the magnitude of R-squared value. Only protein-coding genes with a recurrence value of 2 or greater are shown. *(Continued to the next page)*

mutations in eight out of 11 samples, while two patients harbored adenomatous polyposis coli (*APC*) mutations. *CTNNB1* and *APC* mutation sites of patients are summarized in Fig. 2C. All mutations affected phosphorylation sites necessary for the proper degradation of β-catenin [39-41].

Remarkably, no other mutations in *COSMIC* cancer driver genes were detected, emphasizing the prominent role of the Wnt/β-catenin signaling pathway in desmoid tumor progression [8].

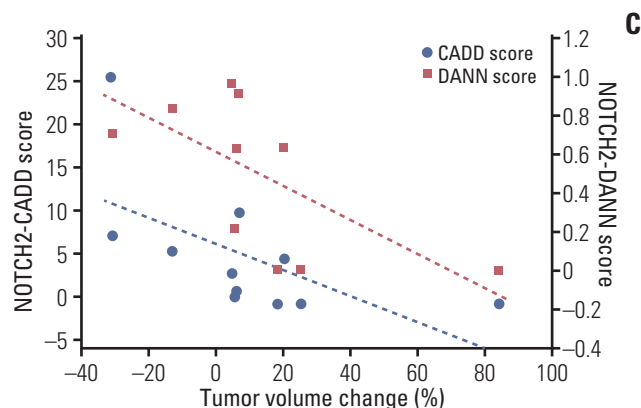**Fig. 3.** *(Continued from the previous page)* (C) CADD scores for *NOTCH2* mutations according to tumor volume changes were plotted with the regression line shown in red (R=–0.716, p=0.013). DANN scores for *NOTCH2* mutations were also plotted with the regression line shown in blue (R=–0.831, p=0.006). Each point represents a patient's sample.

3. Gene-wise recurrence analysis of potential cancer-associated genes

To identify potential cancer-associated mutations in desmoid tumors, we employed gene-wise recurrence analysis of mutations in noncoding regions, according to previously developed method [23]. Briefly, the model assumes that mutations in multiple patients are recurrent if they affect the same gene (Fig. 3A). Recurrently affected genes were defined as those with mutations in at least two samples. This strategy allowed us to evaluate noncoding regions with potentially significant impacts on gene regulation with limited sample size. *NOTCH2*, *RGPD2*, and *ARHGAP11B* were identified as strong candidates (Fig. 3B).

4. Correlation between gene-wise scores and imatinib sensitivity

We examined the association between the change in tumor volume after imatinib treatment and the deleteriousness score of recurrently mutated genes. In case of *NOTCH2*, tumor volume changes were highly correlated with both CADD (R=–0.797, p=0.01) and DANN scores (R=–0.831, p=0.006) (Fig. 3B and C, S7 Table). This correlation was maintained even when two tumor-only samples (patient 11 and 13) were included (Fig. 3C). According to the annotated information of somatic variants in *NOTCH2*, three (patients 3, 5, and 8) and four (patients 9, 11, 13, and 18) variants were intergenic and intronic, respectively, while only one (patient 19) variant was nonsynonymous (S8 Table). Using gnomAD database, we found that the allele frequencies of the *NOTCH2* variants were extremely low (0%-1.13%), indicating that they were likely somatic. These results suggest that the regulation of *NOTCH2* at the gene level may contribute to the desmoid tumor response to imatinib.

5. Regulatory role of *NOTCH2* mutations

To evaluate the regulatory effects of *NOTCH2* mutations, we interrogated RNA sequencing and somatic mutation profiles from PCAWG datasets (n=1,009). For comparison across cancer types, we transformed the *NOTCH2* expression levels to Z-scores within each cancer type and identified samples with *NOTCH2* mutations. Considering the role of *CTNNB1* missense mutations in desmoid tumors [8], we further selected both-*NOTCH2*-*CTNNB1* mutants in the PCAWG data (Fig. 4A, S9 Table).

NOTCH2 expression levels were more highly correlated with CADD scores for both-*NOTCH2*-*CTNNB1* mutation group (R=0.607, p=0.013) than for *NOTCH2* mutation-only group (R=0.178, p=0.01) (Fig. 4B). The same trends were observed when DANN score was used for variant scoring (R=0.467) (Fig. 4C), although the correlation was only marginally significant (p=0.068). These results suggest that genetic interactions between *NOTCH2* noncoding mutations and *CTNNB1* missense mutations may influence the *NOTCH2* expression level.

6. Role of NOTCH family members and *HES1* in imatinib sensitivity

To validate significance of our finding, we analyzed RNA-sequencing data of 29 desmoid tumor patients (Fig. 1, S10 Table). We focused on Notch family members, including *NOTCH2*, and *HES1*, a marker of stemness [42] that has been implicated as a target of Notch signaling pathway [43] and marker of imatinib sensitivity [44]. We first investigated whether expression levels of Notch family members and *HES1* are correlated. We calculated spearman correlation between the genes, and discovered that *NOTCH2* expression was significantly correlated with *HES1* expression (p=0.0091568) while expressions of other Notch genes were not (Fig. 5A). This recapitulates the association between *HES1* and *NOTCH2* detected in whole-genome sequencing analysis. We also noticed that all Notch family members are significantly correlated with each other (S11 Fig.). This suggests that other Notch family members can potentially participate in regulation of *HES1* expression although *NOTCH2* is most directly associated with *HES1*.

Next, we examined whether expression of Notch family members or *HES1* is associated with imatinib response. We classified patients into responders (PR, n=5) or non-responders (SD/progressive disease, n=6) on the basis of clinical implementation, and compared expression values between two groups. Strikingly, we found that none of Notch family members had statistical power to distinguish two groups.
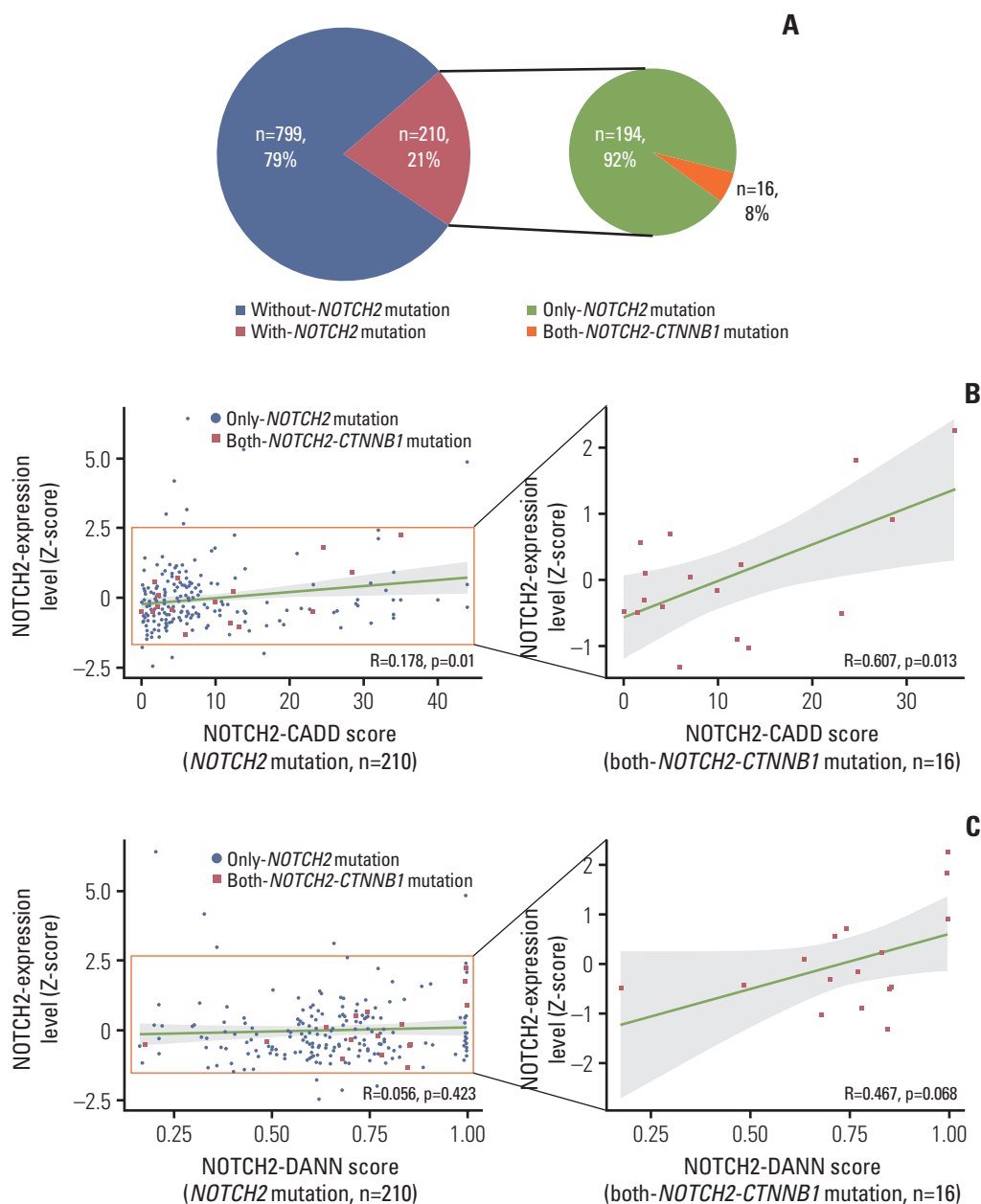
Fig. 4. Correlation between the deleteriousness of *NOTCH2* noncoding-mutations and expression level of *NOTCH2* in Pan-Cancer Analysis of Whole Genomes cohort. (A) Proportions of patients with *NOTCH2* mutations (n=210) and with both *NOTCH2* and *CTNNB1* missense mutations (n=16). (B) Correlation between Combined Annotation-Dependent Depletion (CADD) score and *NOTCH2* expression level in the group with *NOTCH2* mutations (left side) and in selected samples harboring both *NOTCH2* and *CTNNB1* missense mutations (right side). (C) The correlation analysis was repeated using Deleterious Annotation of genetic variants using Neural Networks (DANN) score in the group with *NOTCH2* mutations (left side) and in selected samples with both *NOTCH2* and *CTNNB1* missense mutations (right side).

Intriguingly, *HES1* was significant in discriminating patients' response (p=0.028) (Fig. 5B). This is in accordance with report that overexpression of *HES1* sensitizes cells to imatinib in chronic myeloid leukemia model [44]. Furthermore, we calculated spearman correlation between response rate and

expression levels. Initially, we found no correlation between *HES1* or Notch family genes with tumor volume change, with marginal significance in *HES1* (p=0.070). However, after removing outlier (defined as patient with highest gene expression), we found that *HES1* was significantly correlated
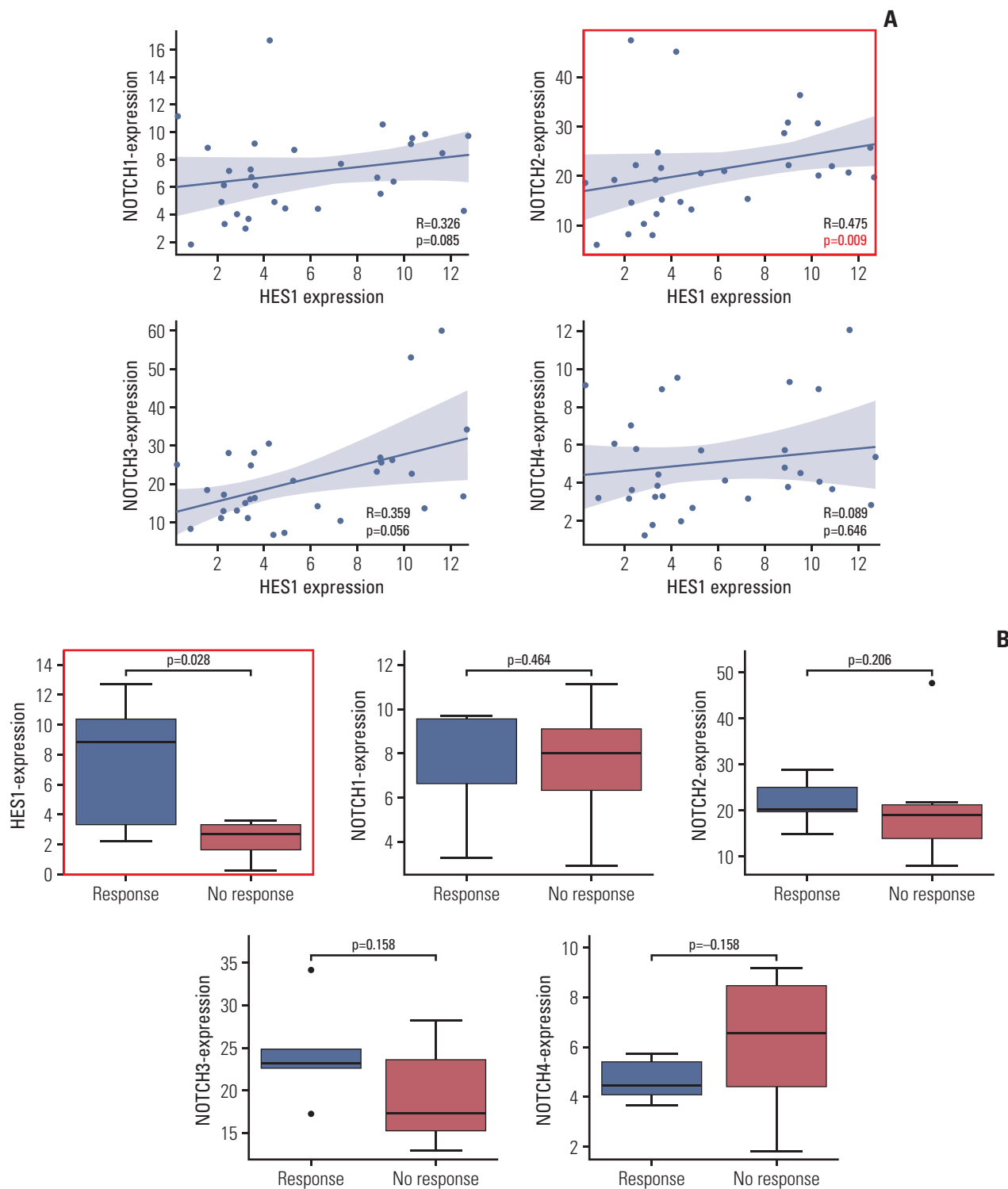
Fig. 5. Expressional association between Notch family and *HES1* genes, and its clinical significance in desmoid tumor samples (n=29). (A) Co-expression between HES1 and one of Notch family genes, including *NOTCH1*, *NOTCH2*, *NOTCH3*, and *NOTCH4*, respectively. Correlation analysis was calculated using spearman and all expression levels are in transcripts per million values. (B) Expressional differences of *HES1*, *NOTCH1*, *NOTCH2*, *NOTCH3*, and *NOTCH4*, between responders (n=5) and non-responders (n=6) after treatment of imatinib. Statistical significance was determined using Mann-Whitney U test. *(Continued to the next page)*
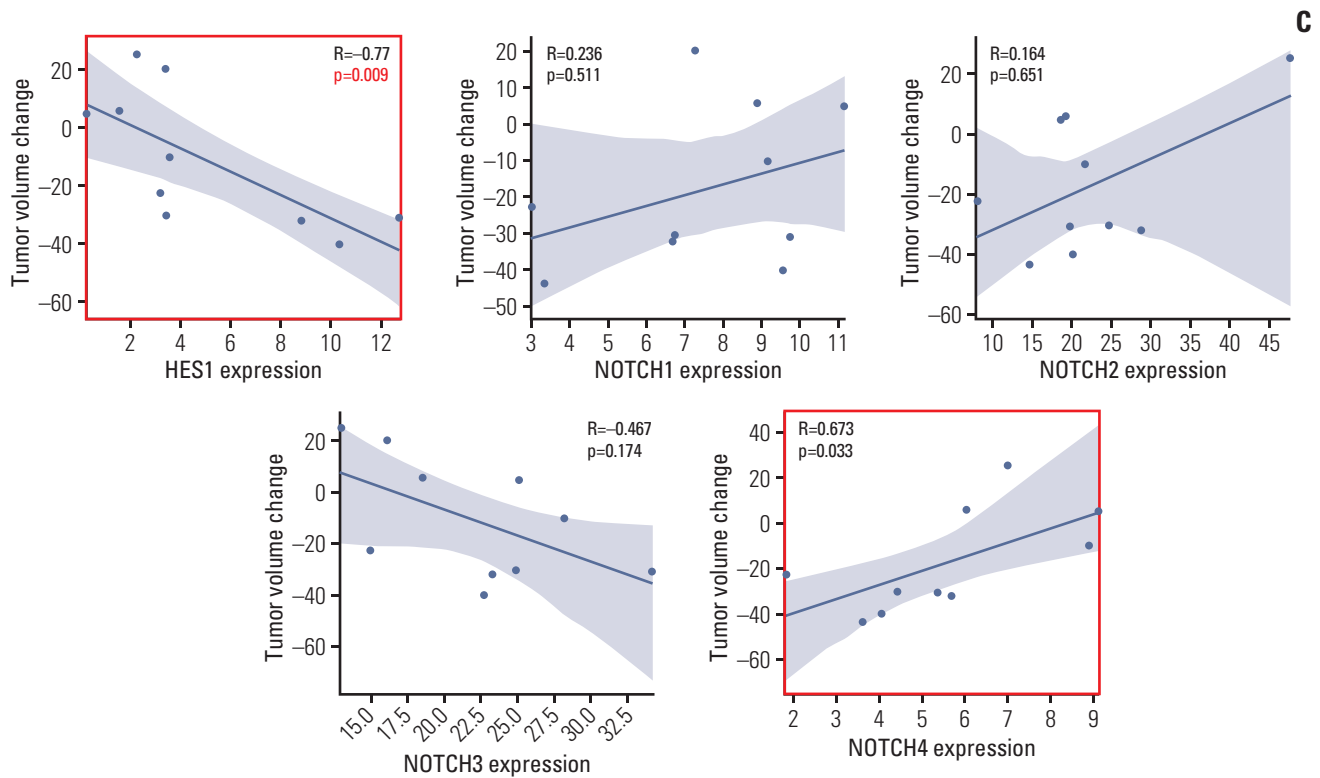
Fig. 5. *(Continued from the previous page)* (C) Correlation between tumor volume change, indicating the imatinib-response, and gene expression level: *HES1* and Notch family members. Plots depict correlation analysis after removing one outlier. All red square lines indicate statistical significance (p < 0.05).

with clinical response (p=0.009) (Fig. 5C). Still, none of Notch members, except *NOTCH4*, achieved statistical significance. Overall, *HES1* was the most significant marker of imatinib sensitivity.

7. Enrichment analysis of response-associated genes

To identify biological pathways that are associated with imatinib sensitivity, we first conducted GSEA between responders and non-responders (Fig. 6A). Differentially expressed genes were enriched in diverse biological pathways including muscle cell cellular homeostasis, negative regulation of myoblast differentiation, and skeletal tissue regeneration, angiogenesis and regulation of oxidative phosphorylation. We also performed enrichment analysis using genes that are significantly correlated with imatinib sensitivity (Fig. 6B). Similar terms, such as fibroblast growth factor binding, muscle cell migration, and oxidative phosphorylation, were enriched. Among these terms, we found that glucose metabolism and mitochondrial respiration have been closely linked to imatinib sensitivity [45] and are upregulated in naïve pluripotent stem cells [46] in previous researches. In addition, angiogenesis is a well-known feature of mesen-

chymal stem cells [47]. Collectively, we propose that these terms, such as oxidative phosphorylation and angiogenesis, and *HES1* all point to the significance of mesenchymal stem cell population that are prone to imatinib in desmoid tumor.

Discussion

Using whole-genome and transcriptome sequencing, we performed integrative molecular characterization of desmoid tumor in patients receiving imatinib treatment. Our analyses suggest *HES1* overexpression, potentially regulated by *NOTCH2*, can serve as a predictor of the clinical response to imatinib in desmoid tumor patients. To our knowledge, this is the first integrative study to characterize molecular determinants of the response to imatinib in desmoid tumor.

Our coding-region analyses recapitulated previous findings on the prevalence of *CTNNB1* and *APC* mutations [48]. Unfortunately, these mutations were not associated with clinical responses to imatinib. However, we discovered that mutations in noncoding regulatory regions of *NOTCH2* are positively correlated with the clinical response to imatinib.
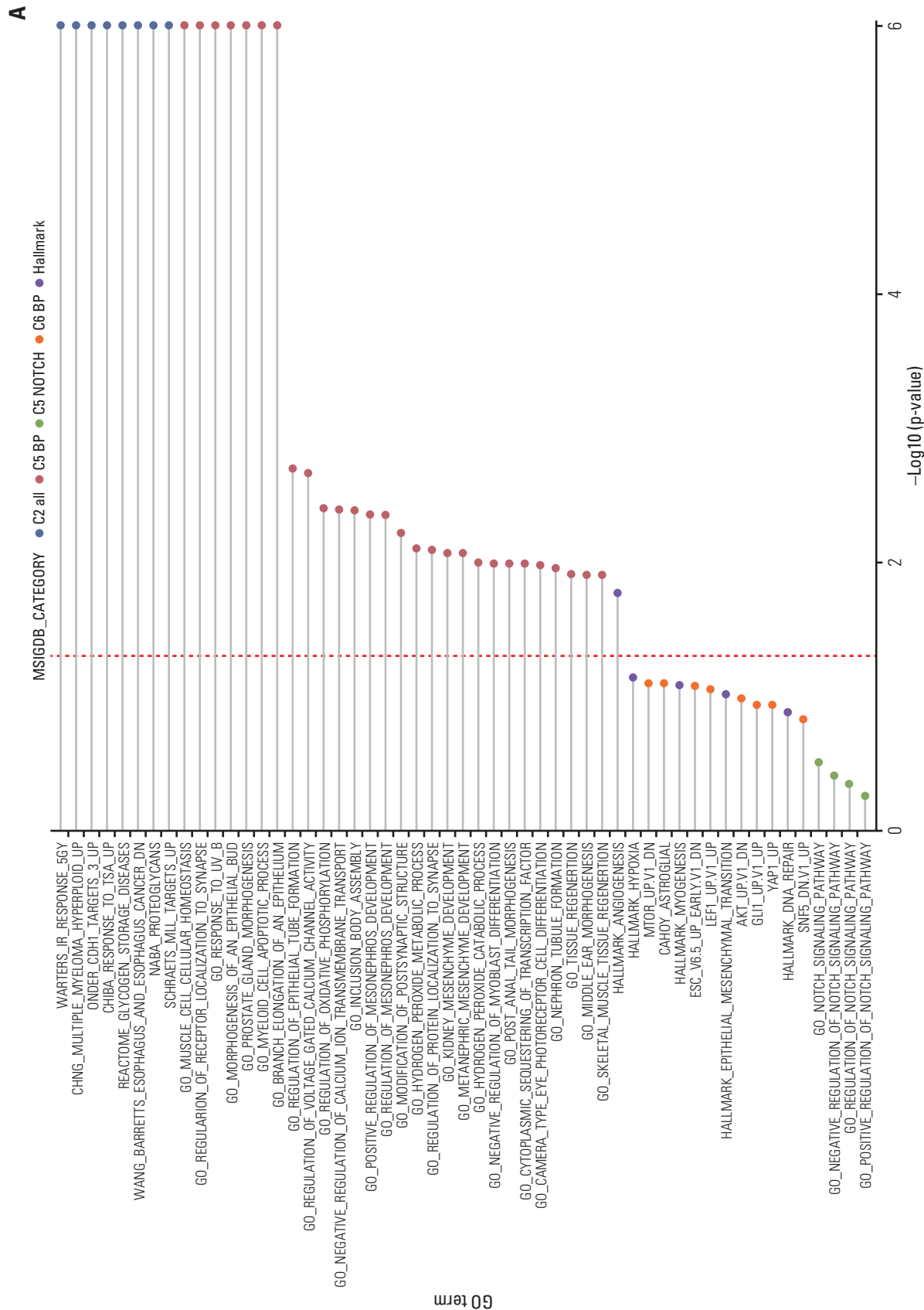
Fig. 6. (A) Gene Set Enrichment Analysis (GSEA) for differential genes with statistical importance (p < 0.05) between responders (n=5) and non-responders (n=6). Gene Ontology terms on y-axis indicate molecular signatures database (MSigDB), of which five gene sets are shown in legend: C2, as curated gene sets; C5 BP, as gene sets from biological process ontology; C5 NOTCH, as gene sets associated with Notch pathway; C6 BP, as oncogenic signatures of biological process; Hallmark, as gene sets to represent specific biological states or processes and show consistent expression. Most significant terms for each category are depicted. (*Continued to the next page*)
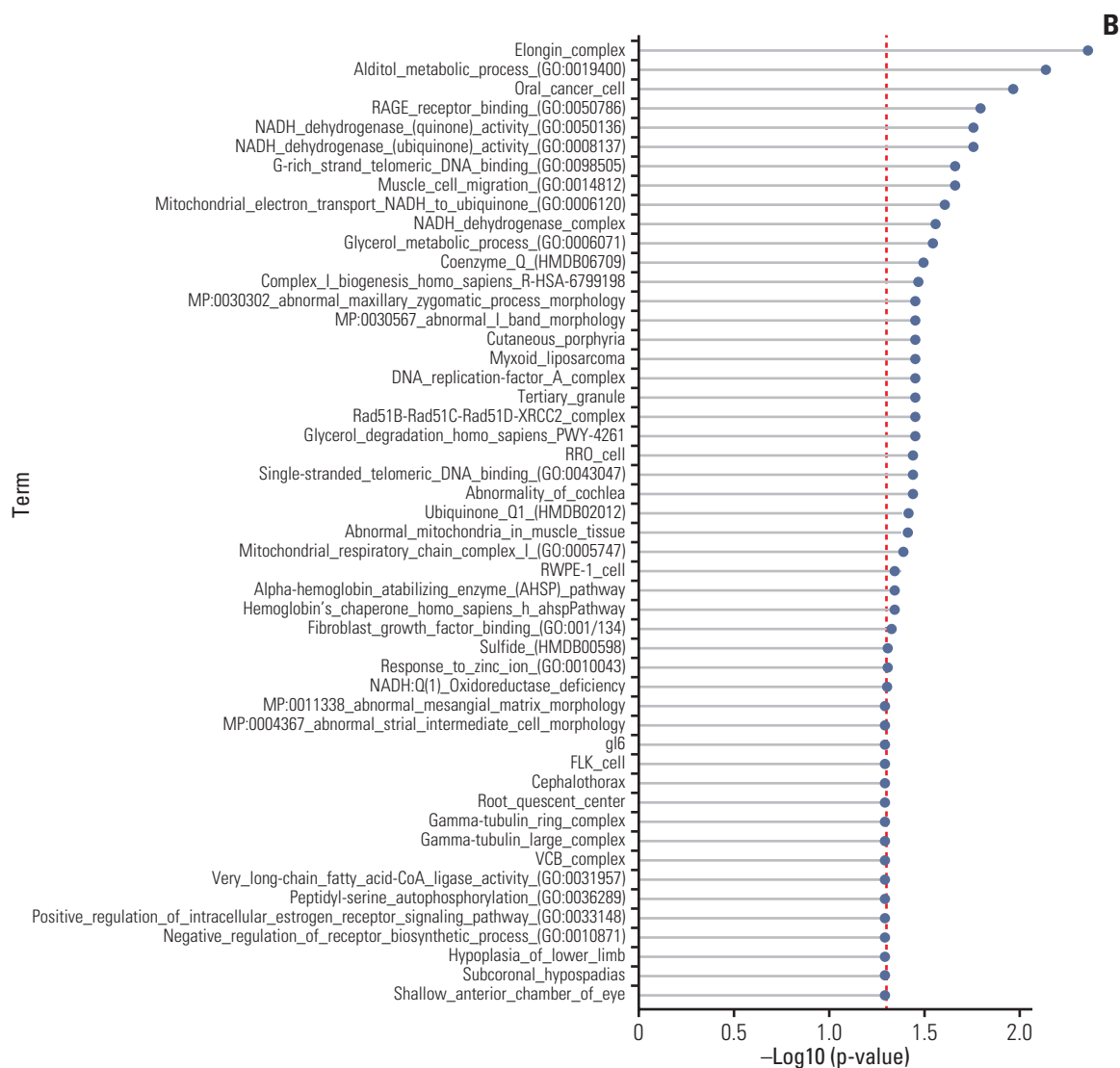
Fig. 6. *(Continued from the previous page)* (B) GSEA result by using EnrichR with genes that are significantly correlated with imatinib sensitivity. Red vertical lines indicate p-value of 0.05.

Moreover, our investigation of PCAWG samples revealed that noncoding mutations in *NOTCH2* regions increase expression. Importantly, *NOTCH2* expression was significantly correlated with *HES1*, and *HES1* was indicative of imatinib sensitivity in our desmoid cohort. We noticed that removal of one outlier restored statistical significance when assessing correlation between *HES1* and tumor volume change. Still, our correlation analysis suggests that *HES1* expression is the major determinant of imatinib sensitivity. Other minor factors of imatinib sensitivity need to be determined to fully elucidate mechanism of imatinib in desmoid tumor. Taken together, we suggest that *HES1* and *NOTCH2* overexpression is a predictor of the anti-cancer effects of imatinib on desmoid tumors.

Our study is not the very first attempt to investigate the significance of Notch signaling in desmoid tumor [43,49]. Based on multiple evidences, small molecule inhibitors, such as γ-secretase inhibitor, siRNA, and monoclonal antibody against Notch pathway were designed to treat desmoid tumor [50]. Studies have confirmed that activation of *NOTCH2* leads to overexpression of *HES1* and are accompanied by proliferation, immature morphology and aggressiveness in acute kidney injury model [51] and hepatocellular carcinoma model [52]. Of note, Notch signaling and *HES1* have been associated with response to imatinib in chronic myeloid leukemia cells [44,53], providing robust evidence for Notch-*HES1* axis in mechanism of imatinib in desmoid tumor. Surprisingly, however, no research reported its asso-

ciation with clinical response of imatinib in desmoid tumor until now.

The mechanism underlying the tumor response to imatinib is still not fully understood. In agreement with our findings, multiple lines of evidence support their significance in desmoid tumor. In a preclinical study, imatinib inhibits Notch signaling by increasing the proteosomal degradation of intracellular Notch. Furthermore, a primary effector of Notch signaling, *HES1*, decreased as the imatinib concentration increased [54]. In a neurodegenerative condition, Alzheimer disease, imatinib results in the dose-dependent inhibition of γ-secretase activity [55]. Similarly, NSAIDs, another standard treatment for desmoid tumors, alter γ-secretase activity [56]. Taken together, these findings support the predictive value of Notch and *HES1* as therapeutic strategy.

The Notch pathway exhibits crosstalk with the Wnt signaling cascade [57] and is involved in the regulation of tumor microenvironments and the maintenance of cancer stem cells [58-60]. With *NOTCH1* activation, desmoid tumors showed high expression levels of *NOTCH1* and its downstream transcription factor *HES1* [43], of which transcriptional activity is dependent on *NOTCH2* [61]. Thus, targeting γ-secretase to prevent Notch cleavage has been suggested as a novel therapeutic approach [62,63]. A phase II trial of the γ-secretase inhibitor PF-03084014 demonstrated a promising efficacy, with a response rate of 29% for patients with progressive desmoid tumors [63]. Furthermore, the efficacy of PF-03084014 is high in tumors with elevated expression of genes in the Notch and Wnt pathways [64].

We sought to explain the increased correlation between *NOTCH2* mutation scores and *NOTCH2* expression levels when considering the *CTNNB1* mutation status. A previous study has shown that the TCF4/β-catenin complex binds to the promoters of Notch signaling pathway genes, including *NOTCH2* [65]. In the absence of the TCF4/β-catenin complex, the transcription machinery cannot be assembled at regulatory regions and fails to induce *NOTCH2* expression, thereby preventing *NOTCH2* regulatory mutations from exerting effects. We speculate that the hyperactivity of the TCF4/β-catenin complex induced by *CTNNB1* msissense mutations leads to the constitutive activation of Notch signaling. This allows *NOTCH2* regulatory mutations to alter gene expression levels, leading to a high correlation between deleteriousness and transcript levels. Further investigations, including functional studies, are needed to validate the mode of action of imatinib.

As mentioned earlier, mutation status of driver genes failed to discriminate patients who will respond to imatinib. We overcame this hurdle with analysis of noncoding mutations, providing rationale to investigate Notch signaling and its downstream target *HES1* to interpret molecular mecha-

nism of imatinib. Thus, significance of noncoding mutation confers huge advantage to whole-genome sequencing data over whole-exome sequencing data. Despite such significance, we acknowledge several limitations of our study. First of all, we are aware that limited sample size hinders more comprehensive study of desmoid tumor. For example, although we were initially unable to obtain statistical significance for *NOTCH2* in Fig. 5B (responder versus nonresponder analysis), removal of outlier restored statistical significance (p-value from 0.2 to 0.07), proving that *NOTCH2* is a biologically meaningful biomarker. Rarity of desmoid tumor obscured the statistical power, and increased sample size will endow power to rescue unrecognized candidates. Also, we admit lack of functional study. Collectively, multiple evidences point out to Notch-*HES1* axis in various studies, its significance in response to imatinib, and role of *HES1* in stemness. Thus, future work should validate both clinical and biological significance of *HES1* in desmoid tumor to gain insight into this aggressive rare tumor.

In conclusion, using whole-genome sequencing with gene-wise recurrence model and transcriptome of desmoid tumor, we propose that overexpression of *NOTCH2* and *HES1* is the marker of sensitivity for the anti-cancer effects of imatinib on desmoid tumors. Our results suggest that *HES1* should especially be considered in clinical settings when using imatinib to treat this rare and challenging disease.

Electronic Supplementary Material
Supplementary materials are available at Cancer Research and Treatment website (https://www.e-crt.org).

Ethical Statement
The study was approved by the institutional review board (IRB No. 2013-1417-001). Retrospective cohort study of 24 additional patients with desmoid tumor was approved by the institutional review board (IRB No. 2020-2244-001). All patients provided written informed consent. This study was conducted in accordance of Declaration of Helsinki.

Author Contributions
Conceived and designed the analysis: Choi JK, Kim HS.
Collected the data: Lee YH, Lee J, Ahn JH, Kim SH (Se Hyun Kim), Kim SH (Seung Hyun Kim), Kim TI, Yun KH, Park YS, Kim JE, Lee KS.
Contributed data or analysis tools: Kwon J, Lee JH.
Performed the analysis: Kwon J, Lee JH.
Wrote the paper: Kwon J, Lee JH.

ORCID iDs

Joonha Kwon ⓘ : https://orcid.org/0000-0002-6607-0277
Jun Hyeong Lee ⓘ : https://orcid.org/0000-0003-2117-0562
Jung Kyoon Choi ⓘ : https://orcid.org/0000-0003-2077-8947
Hyo Song Kim ⓘ : https://orcid.org/0000-0002-0625-9828

References

1. Colombo C, Miceli R, Le Pechoux C, Palassini E, Honore C, Stacchiotti S, et al. Sporadic extra abdominal wall desmoid-type fibromatosis: surgical resection can be safely limited to a minority of patients. Eur J Cancer. 2015;51:186-92.

2. Lev D, Kotilingam D, Wei C, Ballo MT, Zagars GK, Pisters PW, et al. Optimizing treatment of desmoid tumors. J Clin Oncol. 2007;25:1785-91.

3. Spear MA, Jennings LC, Mankin HJ, Spiro IJ, Springfield DS, Gebhardt MC, et al. Individualizing management of aggressive fibromatoses. Int J Radiat Oncol Biol Phys. 1998;40:637-45.

4. Leithner A, Schnack B, Katterschafka T, Wiltschke C, Amann G, Windhager R, et al. Treatment of extra-abdominal desmoid tumors with interferon-alpha with or without tretinoin. J Surg Oncol. 2000;73:21-5.

5. de Camargo VP, Keohan ML, D'Adamo DR, Antonescu CR, Brennan MF, Singer S, et al. Clinical outcomes of systemic therapy for patients with deep fibromatosis (desmoid tumor). Cancer. 2010;116:2258-65.

6. Chao AS, Lai CH, Hsueh S, Chen CS, Yang YC, Soong YK. Successful treatment of recurrent pelvic desmoid tumour with tamoxifen: case report. Hum Reprod. 2000;15:311-3.

7. Azzarelli A, Gronchi A, Bertulli R, Tesoro JD, Baratti D, Pennacchioli E, et al. Low-dose chemotherapy with methotrexate and vinblastine for patients with advanced aggressive fibromatosis. Cancer. 2001;92:1259-64.

8. Penel N, Chibon F, Salas S. Adult desmoid tumors: biology, management and ongoing trials. Curr Opin Oncol. 2017;29: 268-74.

9. Gounder MM, Mahoney MR, Van Tine BA, Ravi V, Attia S, Deshpande HA, et al. Sorafenib for advanced and refractory desmoid tumors. N Engl J Med. 2018;379:2417-28.

10. Heinrich MC, McArthur GA, Demetri GD, Joensuu H, Bono P, Herrmann R, et al. Clinical and molecular studies of the effect of imatinib on advanced aggressive fibromatosis (desmoid tumor). J Clin Oncol. 2006;24:1195-203.

11. Chugh R, Wathen JK, Patel SR, Maki RG, Meyers PA, Schuetze SM, et al. Efficacy of imatinib in aggressive fibromatosis: results of a phase II multicenter Sarcoma Alliance for Research through Collaboration (SARC) trial. Clin Cancer Res. 2010;16:4884-91.

12. Penel N, Le Cesne A, Bui BN, Perol D, Brain EG, Ray-Coquard I, et al. Imatinib for progressive and recurrent aggressive fibromatosis (desmoid tumors): an FNCLCC/French Sarcoma Group phase II trial with a long-term follow-up. Ann Oncol. 2011;22:452-7.

13. Apperley JF, Gardembas M, Melo JV, Russell-Jones R, Bain BJ, Baxter EJ, et al. Response to imatinib mesylate in patients with chronic myeloproliferative diseases with rearrangements of the platelet-derived growth factor receptor beta. N Engl J Med. 2002;347:481-7.

14. Demetri GD, von Mehren M, Blanke CD, Van den Abbeele AD, Eisenberg B, Roberts PJ, et al. Efficacy and safety of imatinib mesylate in advanced gastrointestinal stromal tumors. N Engl J Med. 2002;347:472-80.

15. Druker BJ, Talpaz M, Resta DJ, Peng B, Buchdunger E, Ford JM, et al. Efficacy and safety of a specific inhibitor of the BCR-ABL tyrosine kinase in chronic myeloid leukemia. N Engl J Med. 2001;344:1031-7.

16. Eisenhauer EA, Therasse P, Bogaerts J, Schwartz LH, Sargent D, Ford R, et al. New response evaluation criteria in solid tumours: revised RECIST guideline (version 1.1). Eur J Cancer. 2009;45:228-47.

17. McKenna A, Hanna M, Banks E, Sivachenko A, Cibulskis K, Kernytsky A, et al. The Genome Analysis Toolkit: a MapReduce framework for analyzing next-generation DNA sequencing data. Genome Res. 2010;20:1297-303.

18. Li H, Durbin R. Fast and accurate short read alignment with Burrows-Wheeler transform. Bioinformatics. 2009;25:1754-60.

19. Cibulskis K, Lawrence MS, Carter SL, Sivachenko A, Jaffe D, Sougnez C, et al. Sensitive detection of somatic point mutations in impure and heterogeneous cancer samples. Nat Biotechnol. 2013;31:213-9.

20. Yang H, Wang K. Genomic variant annotation and prioritization with ANNOVAR and wANNOVAR. Nat Protoc. 2015; 10:1556-66.

21. Thorvaldsdottir H, Robinson JT, Mesirov JP. Integrative Genomics Viewer (IGV): high-performance genomics data visualization and exploration. Brief Bioinform. 2013;14:178-92.

22. Lek M, Karczewski KJ, Minikel EV, Samocha KE, Banks E, Fennell T, et al. Analysis of protein-coding genetic variation in 60,706 humans. Nature. 2016;536:285-91.

23. Kim K, Jang K, Yang W, Choi EY, Park SM, Bae M, et al. Chromatin structure-based prediction of recurrent noncoding mutations in cancer. Nat Genet. 2016;48:1321-6.

24. Vogelstein B, Papadopoulos N, Velculescu VE, Zhou S, Diaz LA Jr, Kinzler KW. Cancer genome landscapes. Science. 2013; 339:1546-58.

25. Sanyal A, Lajoie BR, Jain G, Dekker J. The long-range interaction landscape of gene promoters. Nature. 2012;489:109-13.

26. Harrow J, Frankish A, Gonzalez JM, Tapanari E, Diekhans

M, Kokocinski F, et al. GENCODE: the reference human genome annotation for The ENCODE Project. Genome Res. 2012;22:1760-74.

27. Kircher M, Witten DM, Jain P, O'Roak BJ, Cooper GM, Shendure J. A general framework for estimating the relative pathogenicity of human genetic variants. Nat Genet. 2014;46:310-5.

28. Quang D, Chen Y, Xie X. DANN: a deep learning approach for annotating the pathogenicity of genetic variants. Bioinformatics. 2015;31:761-3.

29. ICGC/TCGA Pan-Cancer Analysis of Whole Genomes Consortium. Pan-cancer analysis of whole genomes. Nature. 2020;578:82-93.

30. Martin M. Cutadapt removes adapter sequences from high-throughput sequencing reads. EMBnet J. 2011;17:10-2.

31. Dobin A, Davis CA, Schlesinger F, Drenkow J, Zaleski C, Jha S, et al. STAR: ultrafast universal RNA-seq aligner. Bioinformatics. 2013;29:15-21.

32. Li B, Dewey CN. RSEM: accurate transcript quantification from RNA-Seq data with or without a reference genome. BMC Bioinformatics. 2011;12:323.

33. Wang L, Wang S, Li W. RSeQC: quality control of RNA-seq experiments. Bioinformatics. 2012;28:2184-5.

34. Ewels P, Magnusson M, Lundin S, Kaller M. MultiQC: summarize analysis results for multiple tools and samples in a single report. Bioinformatics. 2016;32:3047-8.

35. Kuleshov MV, Jones MR, Rouillard AD, Fernandez NF, Duan Q, Wang Z, et al. Enrichr: a comprehensive gene set enrichment analysis web server 2016 update. Nucleic Acids Res. 2016;44:W90-7.

36. Subramanian A, Tamayo P, Mootha VK, Mukherjee S, Ebert BL, Gillette MA, et al. Gene set enrichment analysis: a knowledge-based approach for interpreting genome-wide expression profiles. Proc Natl Acad Sci U S A. 2005;102:15545-50.

37. Rosenthal R, McGranahan N, Herrero J, Taylor BS, Swanton C. DeconstructSigs: delineating mutational processes in single tumors distinguishes DNA repair deficiencies and patterns of carcinoma evolution. Genome Biol. 2016;17:31.

38. Forbes SA, Beare D, Boutselakis H, Bamford S, Bindal N, Tate J, et al. COSMIC: somatic cancer genetics at high-resolution. Nucleic Acids Res. 2017;45:D777-83.

39. Le Guellec S, Soubeyran I, Rochaix P, Filleron T, Neuville A, Hostein I, et al. CTNNB1 mutation analysis is a useful tool for the diagnosis of desmoid tumors: a study of 260 desmoid tumors and 191 potential morphologic mimics. Mod Pathol. 2012;25:1551-8.

40. Mullen JT, DeLaney TF, Rosenberg AE, Le L, Iafrate AJ, Kobayashi W, et al. Beta-catenin mutation status and outcomes in sporadic desmoid tumors. Oncologist. 2013;18:1043-9.

41. Lazar AJ, Tuvin D, Hajibashi S, Habeeb S, Bolshakov S, Mayordomo-Aranda E, et al. Specific mutations in the beta-catenin gene (CTNNB1) correlate with local recurrence in sporadic desmoid tumors. Am J Pathol. 2008;173:1518-27.

42. Liu ZH, Dai XM, Du B. Hes1: a key role in stemness, metastasis and multidrug resistance. Cancer Biol Ther. 2015;16:353-9.

43. Carothers AM, Rizvi H, Hasson RM, Heit YI, Davids JS, Bertagnolli MM, et al. Mesenchymal stromal cell mutations and wound healing contribute to the etiology of desmoid tumors. Cancer Res. 2012;72:346-55.

44. Eskandari S, Yazdanparast R. Overexpression of Hes1 is involved in sensitization of K562 cells to Imatinib. J Cell Biochem. 2019;120:10128-36.

45. Bouitbir J, Panajatovic MV, Frechard T, Roos NJ, Krahenbuhl S. Imatinib and dasatinib provoke mitochondrial dysfunction leading to oxidative stress in C2C12 myotubes and human RD cells. Front Pharmacol. 2020;11:1106.

46. Shyh-Chang N, Ng HH. The metabolic programming of stem cells. Genes Dev. 2017;31:336-46.

47. Watt SM, Gullo F, van der Garde M, Markeson D, Camicia R, Khoo CP, et al. The angiogenic properties of mesenchymal stem/stromal cells and their therapeutic potential. Br Med Bull. 2013;108:25-53.

48. Escobar C, Munker R, Thomas JO, Li BD, Burton GV. Update on desmoid tumors. Ann Oncol. 2012;23:562-9.

49. Messersmith WA, Shapiro GI, Cleary JM, Jimeno A, Dasari A, Huang B, et al. A Phase I, dose-finding study in patients with advanced solid malignancies of the oral gamma-secretase inhibitor PF-03084014. Clin Cancer Res. 2015;21:60-7.

50. Timbergen MJ, Smits R, Grunhagen DJ, Verhoef C, Sleijfer S, Wiemer EA. Activated signaling pathways and targeted therapies in desmoid-type fibromatosis: a literature review. Front Oncol. 2019;9:397.

51. Kobayashi T, Terada Y, Kuwana H, Tanaka H, Okado T, Kuwahara M, et al. Expression and function of the Delta-1/Notch-2/Hes-1 pathway during experimental acute kidney injury. Kidney Int. 2008;73:1240-50.

52. Hayashi Y, Osanai M, Lee GH. NOTCH2 signaling confers immature morphology and aggressiveness in human hepatocellular carcinoma cells. Oncol Rep. 2015;34:1650-8.

53. Aljedai A, Buckle AM, Hiwarkar P, Syed F. Potential role of Notch signalling in CD34+ chronic myeloid leukaemia cells: cross-talk between Notch and BCR-ABL. PLoS One. 2015; 10:e0123016.

54. Callahan R, Chestnut BA, Raafat A. Original research: featured article: imatinib mesylate (Gleevec) inhibits Notch and c-Myc signaling: five-day treatment permanently rescues mammary development. Exp Biol Med (Maywood). 2017; 242:53-67.

55. Netzer WJ, Dou F, Cai D, Veach D, Jean S, Li Y, et al. Gleevec inhibits beta-amyloid production but not Notch cleavage. Proc Natl Acad Sci U S A. 2003;100:12444-9.

56. Weggen S, Eriksen JL, Das P, Sagi SA, Wang R, Pietrzik CU, et al. A subset of NSAIDs lower amyloidogenic Abeta42 independently of cyclooxygenase activity. Nature. 2001;414:212-6.

57. Kim HA, Koo BK, Cho JH, Kim YY, Seong J, Chang HJ, et al. Notch1 counteracts WNT/beta-catenin signaling through chromatin modification in colorectal cancer. J Clin Invest. 2012;122:3248-59.

58. Benedito R, Hellstrom M. Notch as a hub for signaling in angiogenesis. Exp Cell Res. 2013;319:1281-8.

59. Batlle E, Clevers H. Cancer stem cells revisited. Nat Med. 2017;23:1124-34.

60. Meurette O, Mehlen P. Notch signaling in the tumor microen-

vironment. Cancer Cell. 2018;34:536-48.

61. Espinosa L, Ingles-Esteve J, Aguilera C, Bigas A. Phosphorylation by glycogen synthase kinase-3 beta down-regulates Notch activity, a link for Notch and Wnt pathways. J Biol Chem. 2003;278:32227-35.

62. Shang H, Braggio D, Lee YJ, Al Sannaa GA, Creighton CJ, Bolshakov S, et al. Targeting the Notch pathway: a potential therapeutic approach for desmoid tumors. Cancer. 2015; 121:4088-96.

63. Kummar S, O'Sullivan Coyne G, Do KT, Turkbey B, Meltzer PS, Polley E, et al. Clinical activity of the gamma-secretase inhibitor PF-03084014 in adults with desmoid tumors (aggressive fibromatosis). J Clin Oncol. 2017;35:1561-9.

64. Arcaroli JJ, Quackenbush KS, Purkey A, Powell RW, Pitts TM, Bagby S, et al. Tumours with elevated levels of the Notch and Wnt pathways exhibit efficacy to PF-03084014, a gamma-secretase inhibitor, in a preclinical colorectal explant model. Br J Cancer. 2013;109:667-75.

65. Ungerback J, Elander N, Grunberg J, Sigvardsson M, Soderkvist P. The Notch-2 gene is regulated by Wnt signaling in cultured colorectal cancer cells. PLoS One. 2011;6:e17957.